

MANCHESTER
1824

The University of Manchester

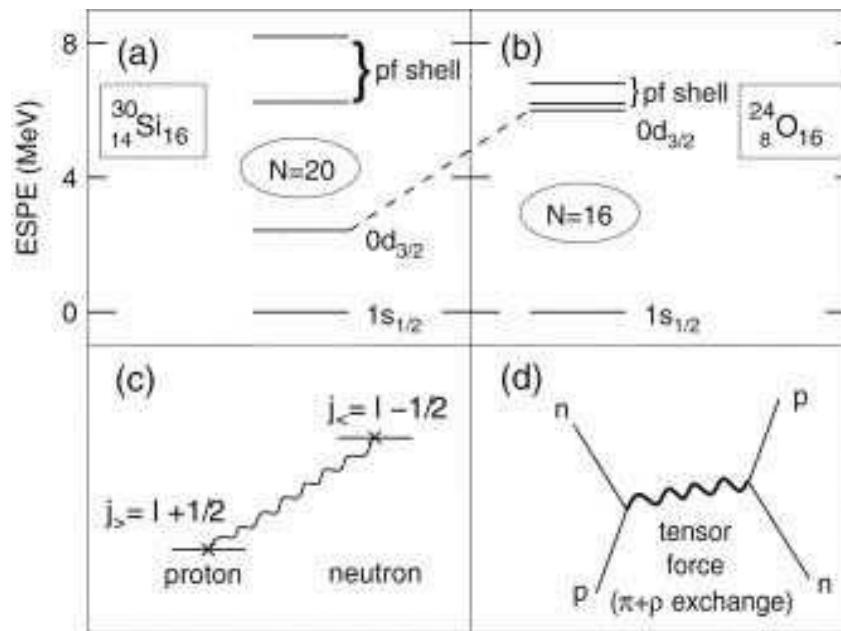
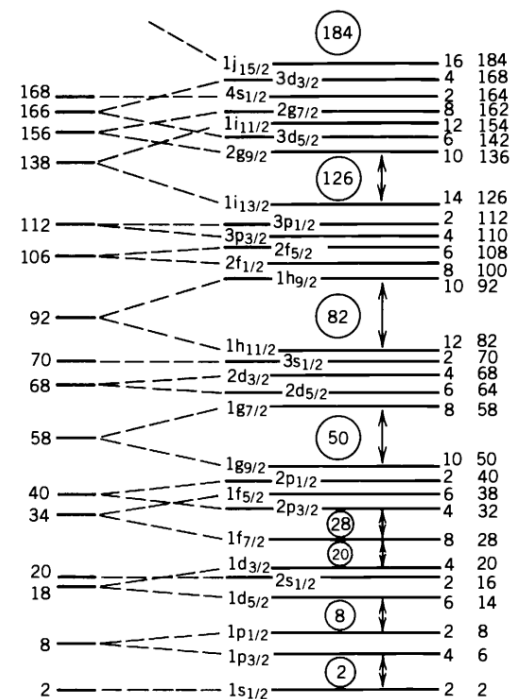


The evolution of single-particle states along
 $N=127$ using the $d(^{212}\text{Rn}, p)^{213}\text{Rn}$ reaction at the
ISOLDE Solenoidal Spectrometer (ISS)

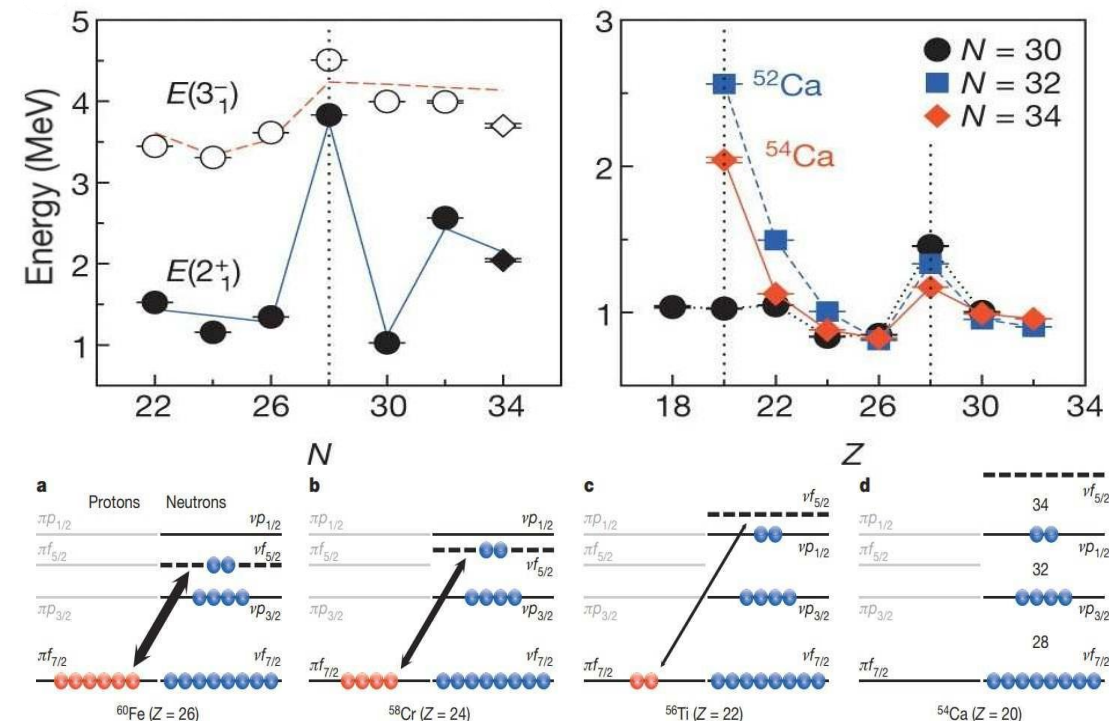
Daniel Clarke
ISOLDE Workshop and Users Meeting 2022

Single-particle evolution in nuclei

- Far from stability, shell closures have been shown to evolve for systems with imbalances of protons and neutrons
- Studies of light neutron-rich system have led to the discovery of new shell closures

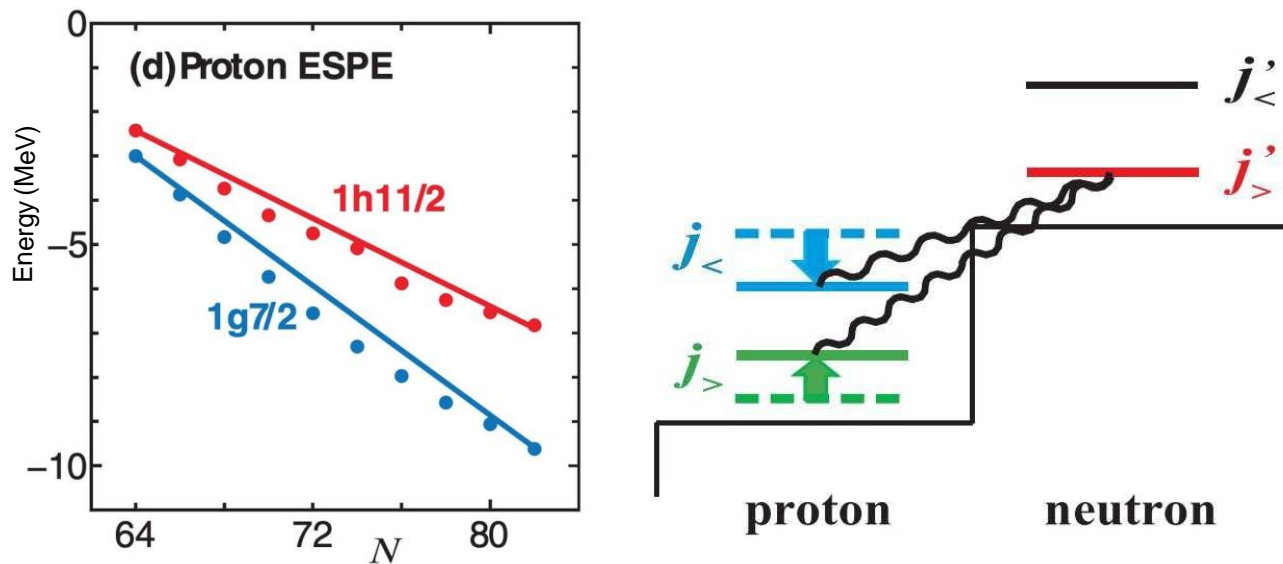


T.Otsuka and D. Abe Prog. In Particle and Nuclear Physics 59 425 (2007)

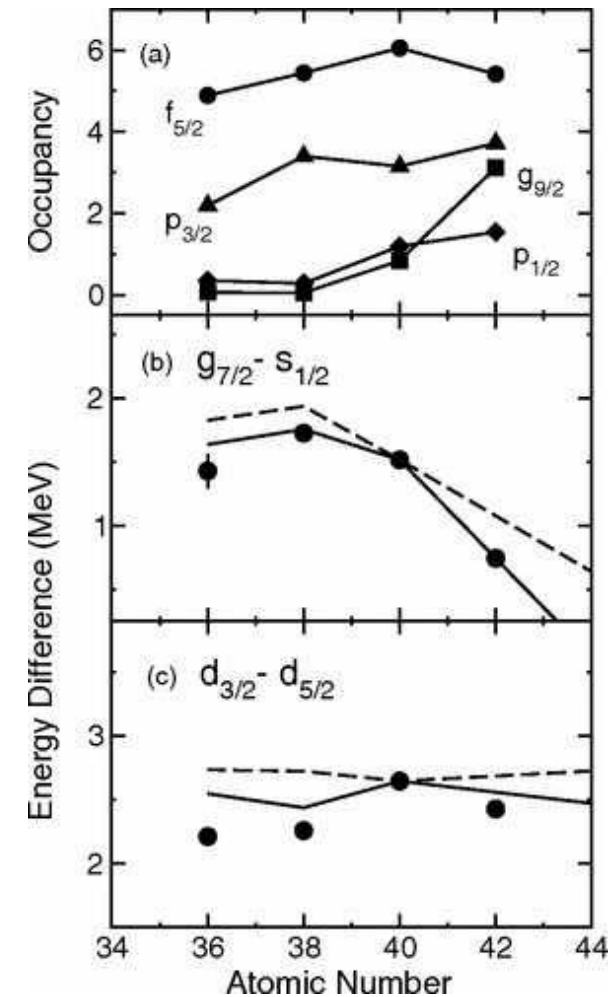


D. Steppenbeck et al, Nature 502 207 (2013)

- In heavier stable nuclei trends have also been observed, particularly in high- j states as other high- j states fill with nucleons
- Studying chains of isotopes/isotones near closed shells have pointed to the inclusion of a tensor interaction to explain systematics



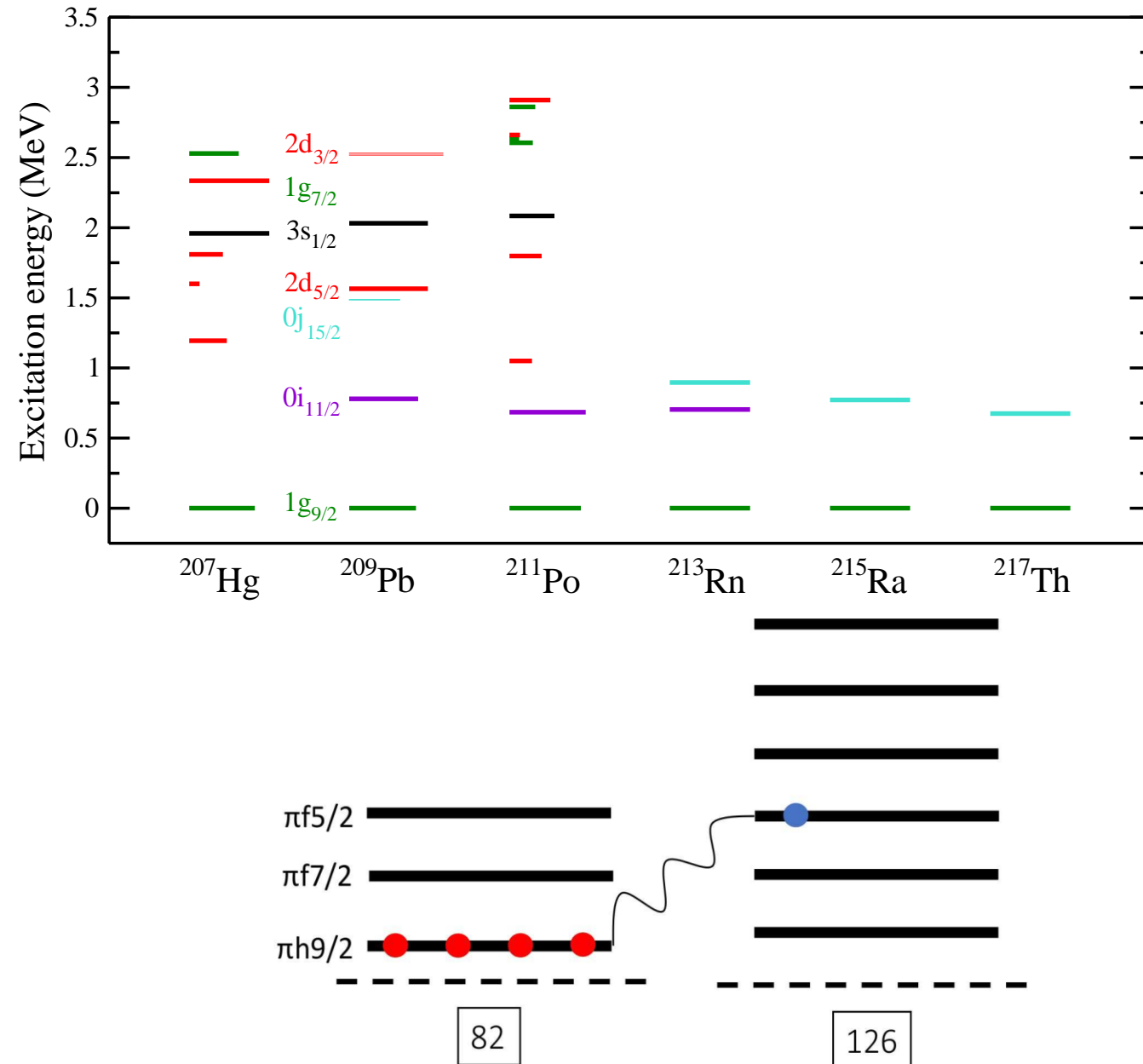
Otsuka et al. Phys. Rev. Lett. 95, 232502 (2005)



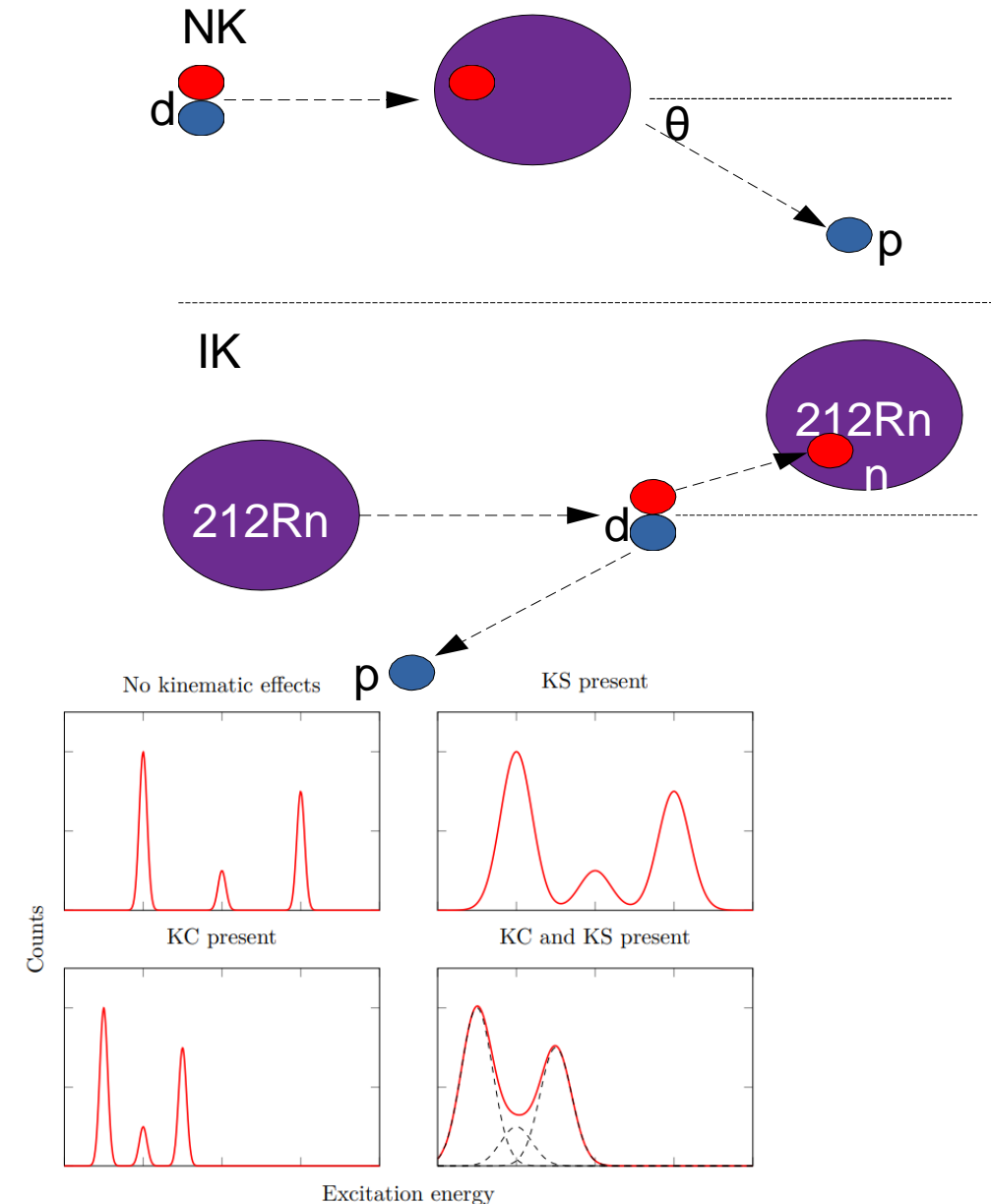
D.K. Sharp et al, Phys.Rev.C 87 014312 (2013)

Single-particle evolution along N=126

- Radioactive beams at HIE-ISOLDE allow new closed-shell systems to be studied
- Studies can be extended to N=126 isotones
- Currently, spectroscopic information on states up to Z=84 (^{211}Po) is known
- The location of nuclei with one neutron outside the N=126 closed shell makes them ideal testing grounds for modern shell-model calculations
- Aim is to probe the strength of neutron orbitals in this region which will be interacting with protons in the $\pi h_{9/2}$ orbital



- Information:
 - Yields - cross sections
 - θ - angular momentum
 - Proton energy - excitation energy of nucleus.
- $d(^{212}\text{Rn}, p)^{213}\text{Rn}$:
 - Need to consider lab to CM transformations
- Problems:
 - Kinematic compression – reduces energy difference between states
 - Kinematic shift – broadens peaks



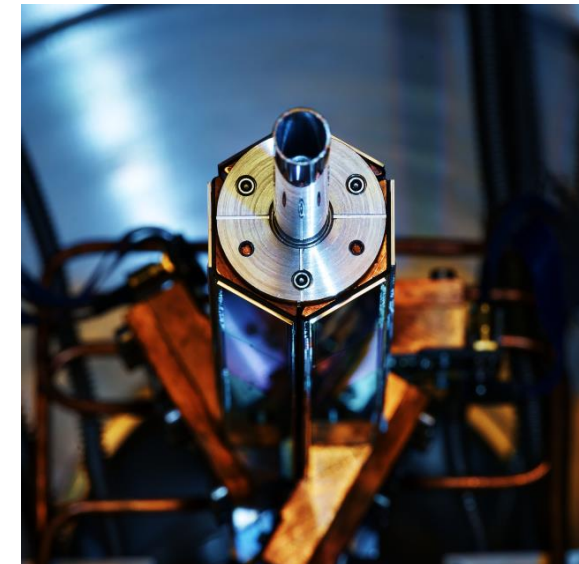
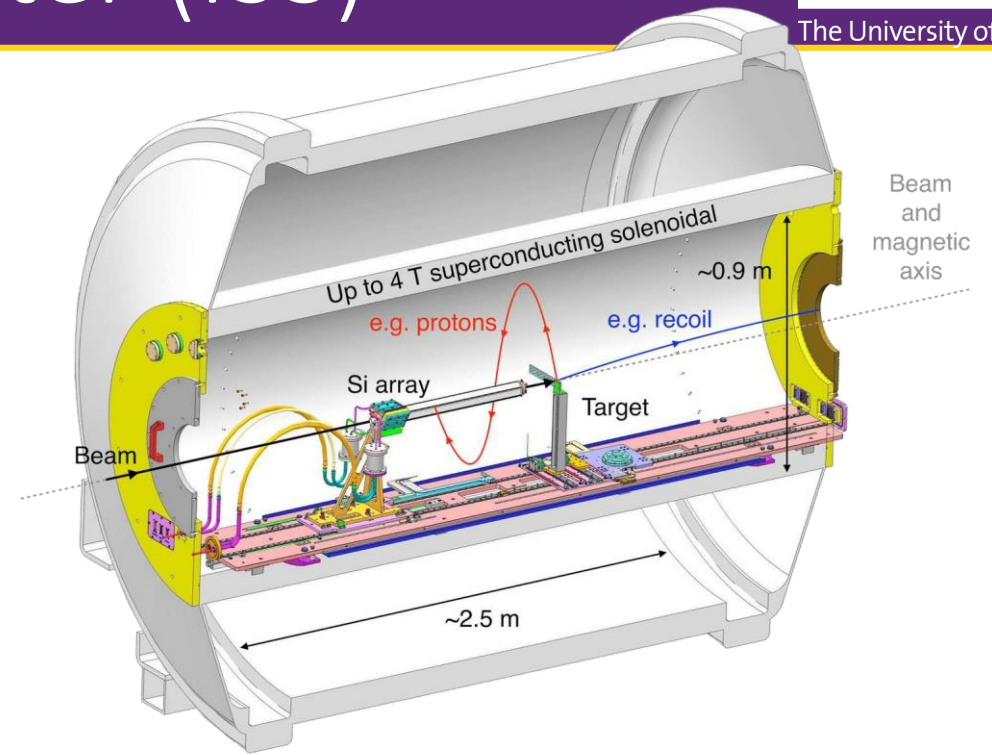
ISOLDE Solenoidal Spectrometer (ISS)

- Potential solution using a solenoid (2.5 T).
- Particles from target follow helical orbits and return to the axis after one cyclotron period

$$T_{cyc} = \frac{2\pi r}{v_{\perp}} = \frac{2\pi m}{qB}$$

- Measure protons in position-sensitive array
- Position, $E_{lab} \propto E_{cm}$.
- No compression in the solenoid – better resolution

$$E_{cm} = E_{lab} + \frac{m}{2} V_{cm}^2 - \frac{mV_{cm}z}{T_{cyc}}$$

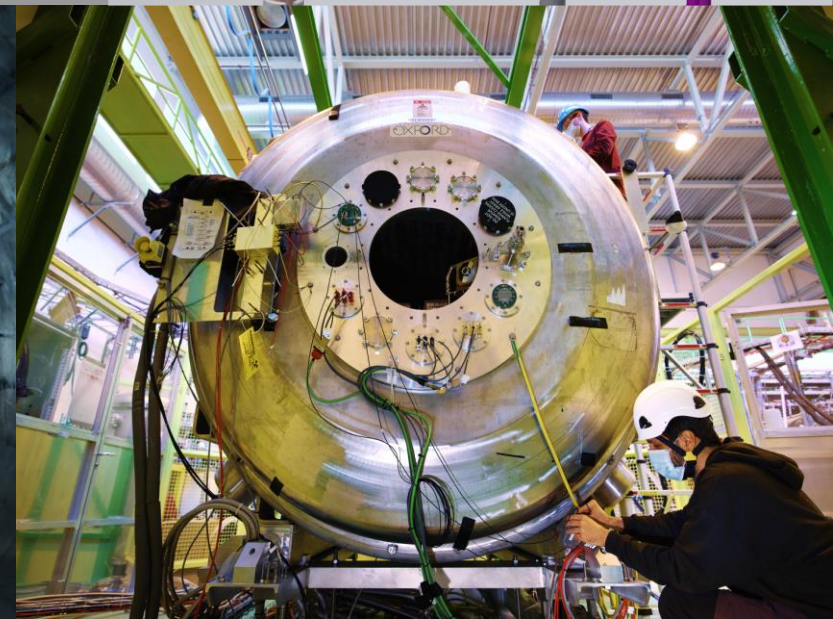
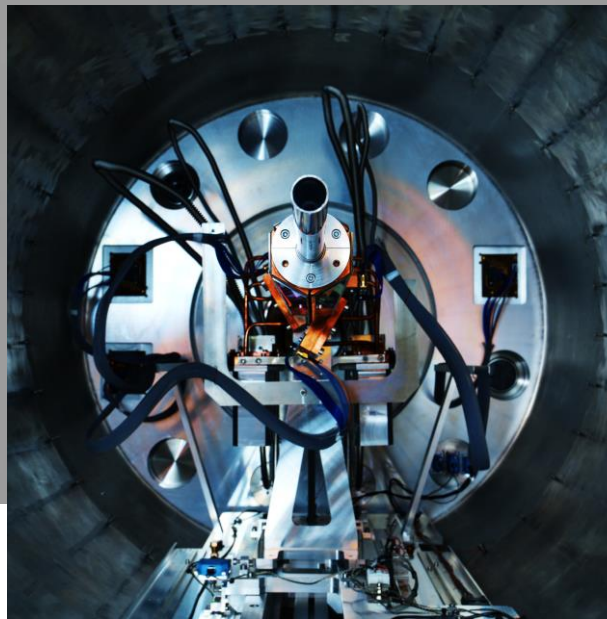
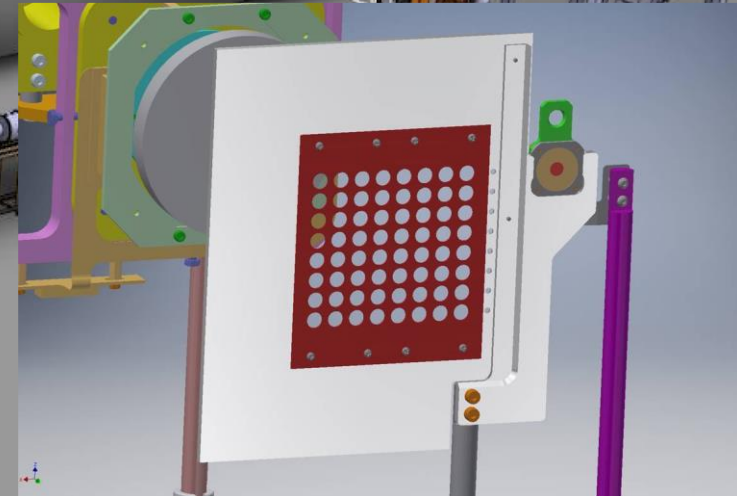
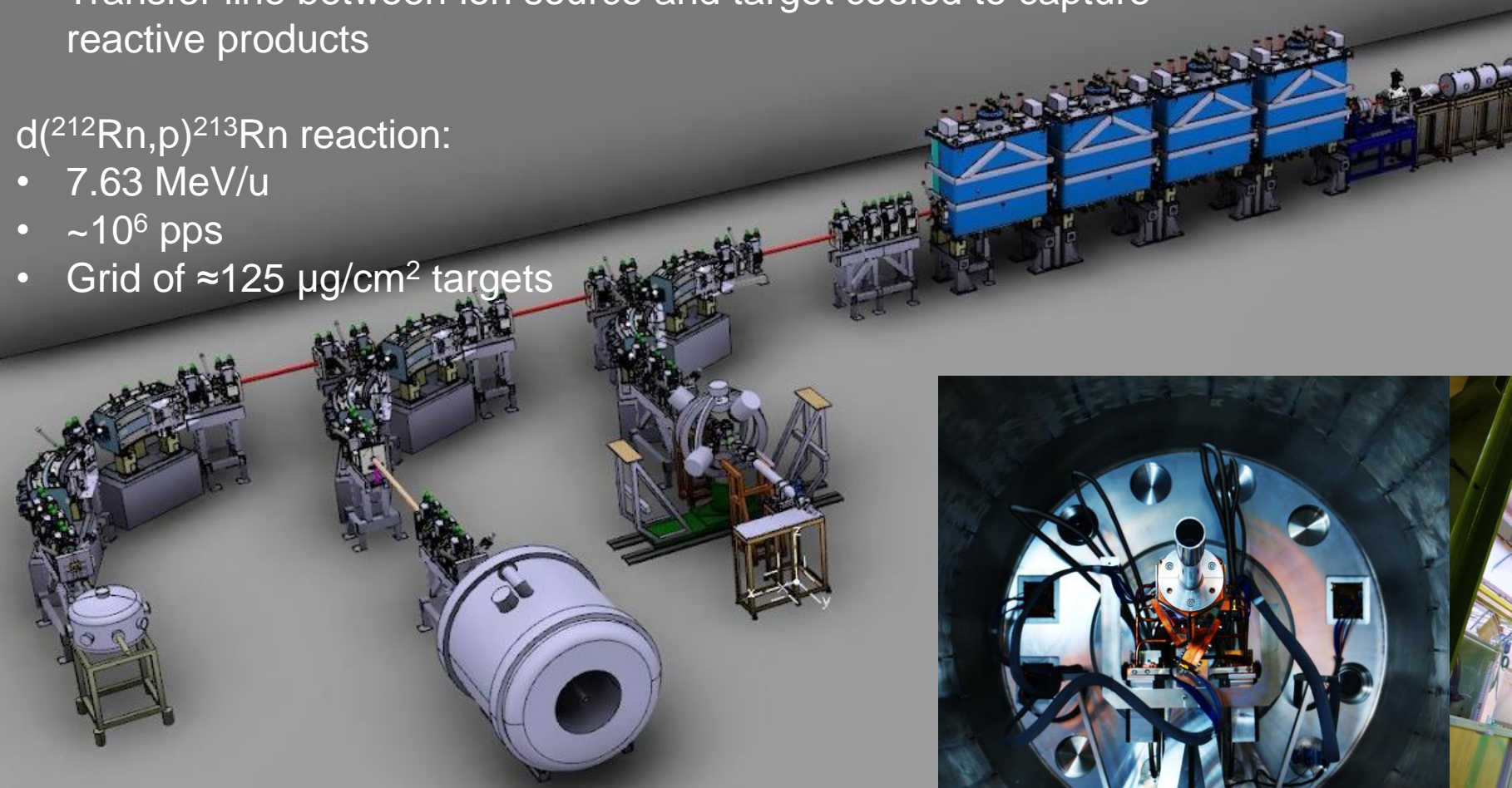


Experiment performed using HIE-ISOLDE:

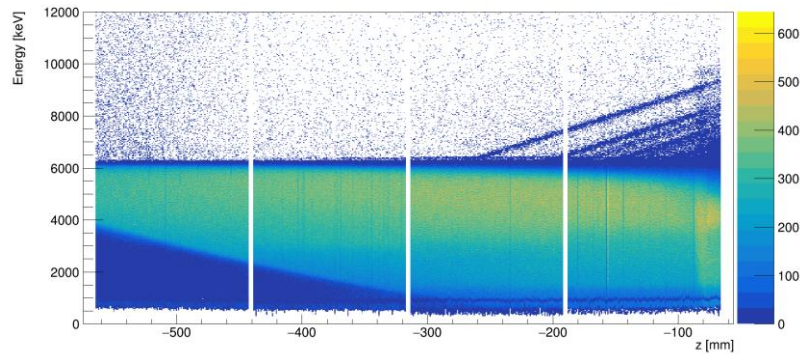
- Protons from the PSB (1.4 GeV) impinged on a heated UC_x target
- VADIS ion-source
- Transfer line between ion source and target cooled to capture reactive products

$d(^{212}\text{Rn},p)^{213}\text{Rn}$ reaction:

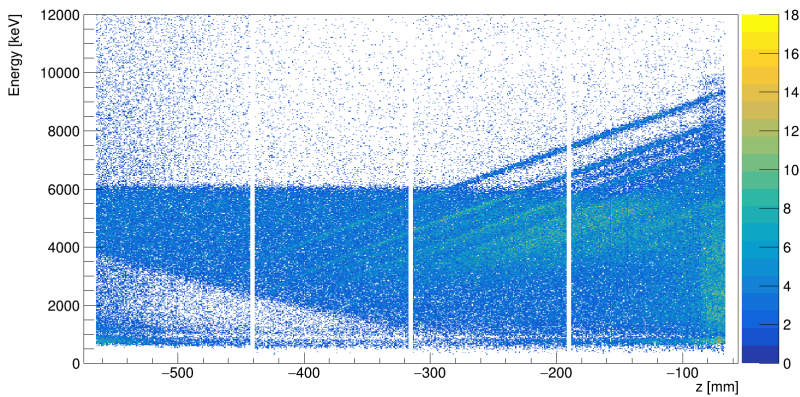
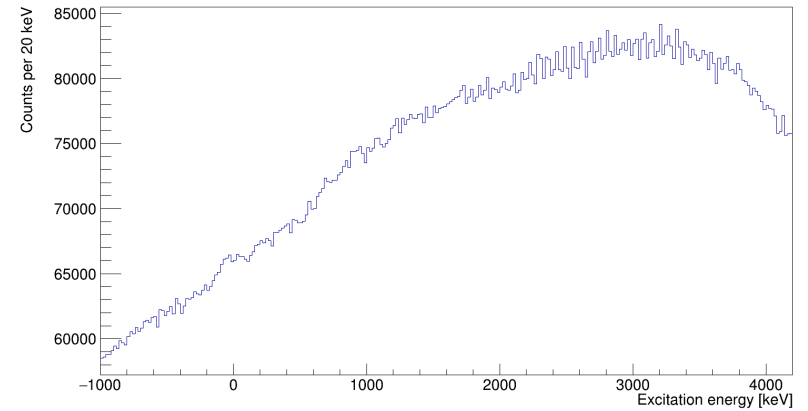
- 7.63 MeV/u
- $\sim 10^6$ pps
- Grid of $\approx 125 \mu\text{g}/\text{cm}^2$ targets



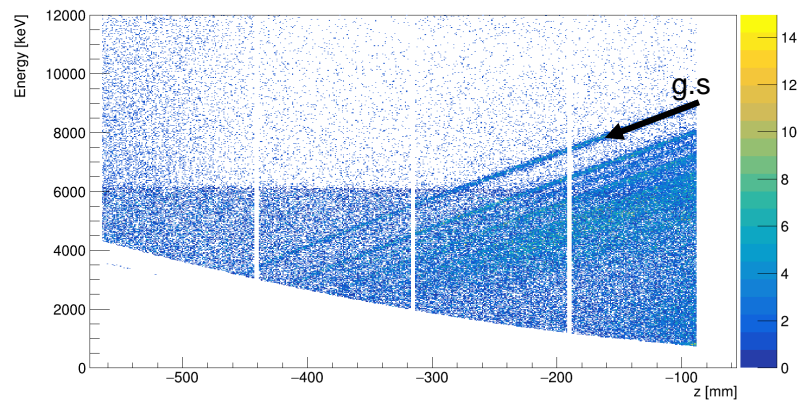
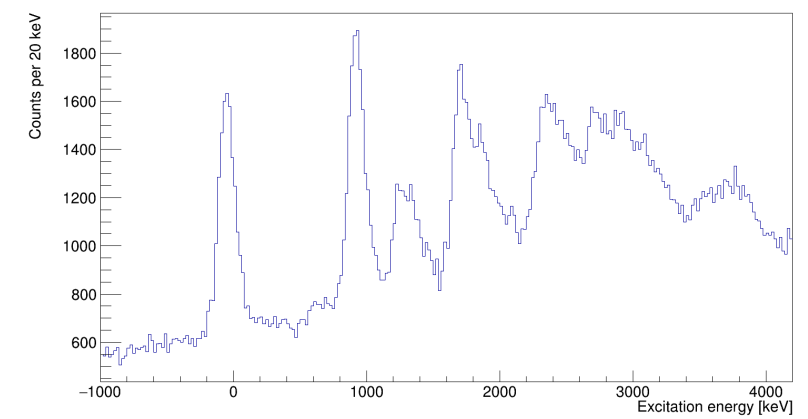
Preliminary data analysis



Singles



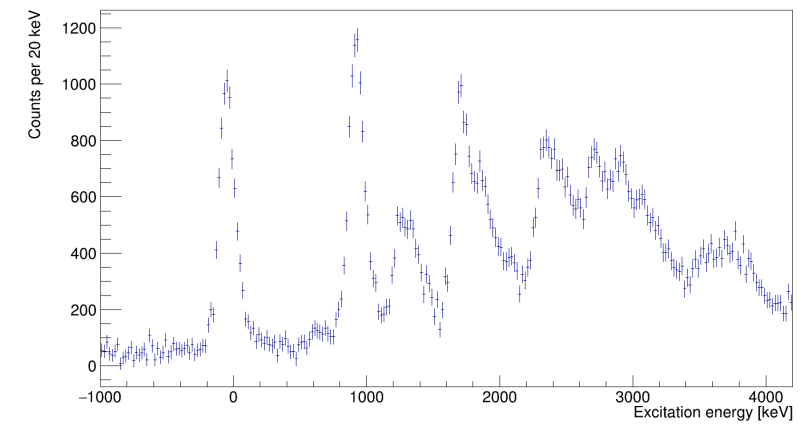
Gating on EBIS-on time



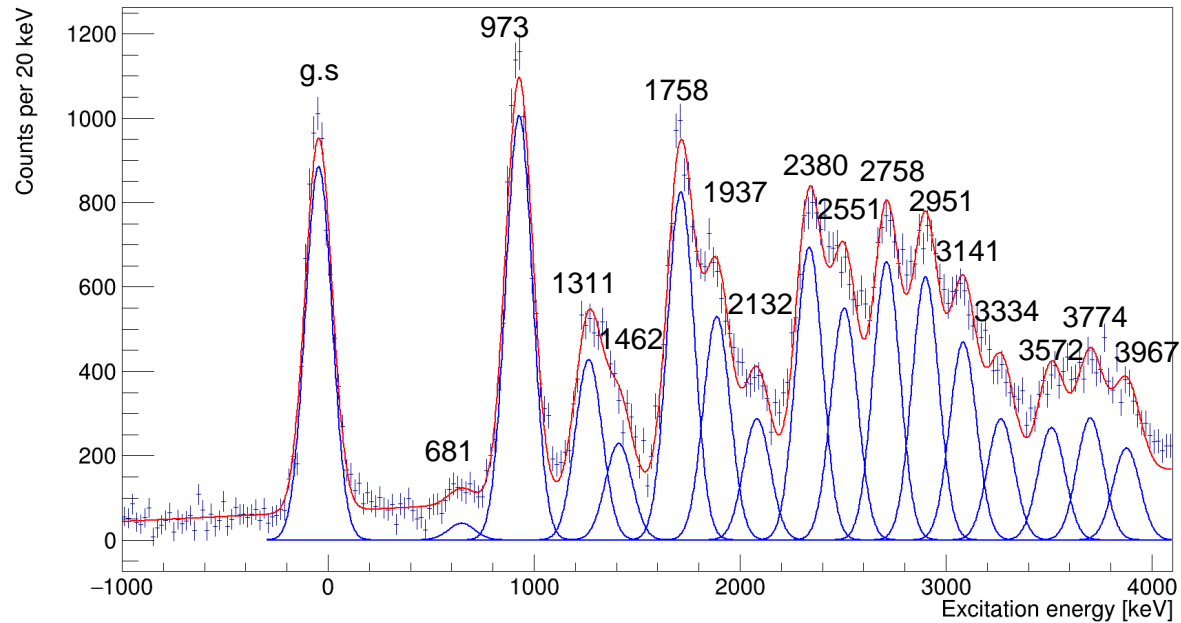
Subtracting EBIS-off time



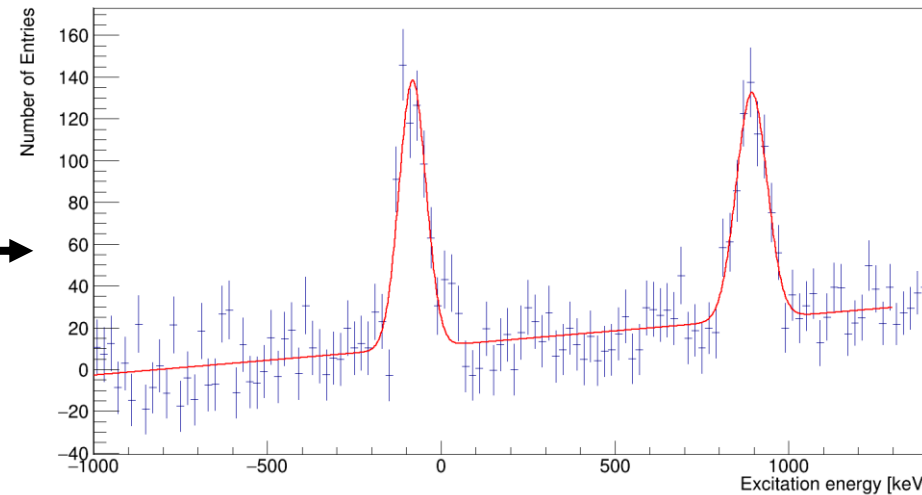
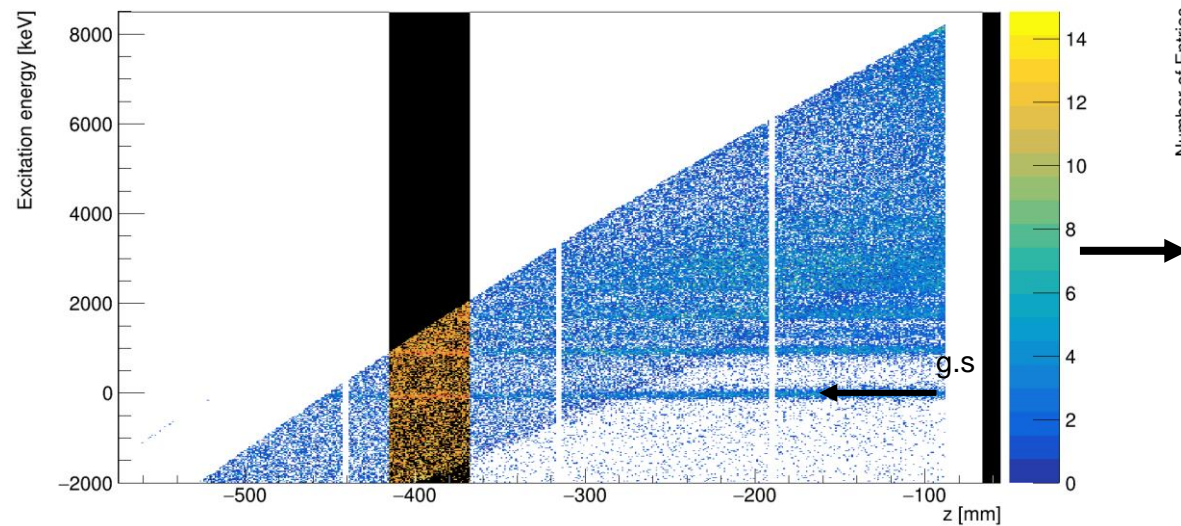
θ_{cm} and z cuts



Preliminary excitation energy spectrum



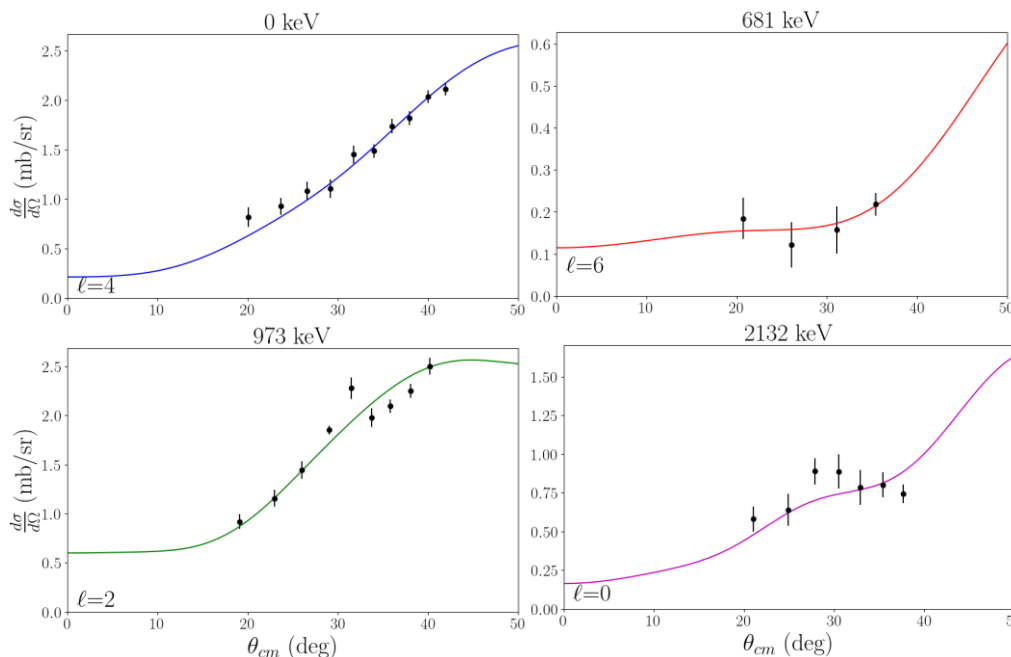
- Identified 17 states in ^{213}Rn up to ~ 4 MeV
- Projected excitation energies
- Regions in z map to θ_{cm}
- Extracted yields of states
- Measured cross sections



$$\frac{d\sigma}{d\Omega} = \frac{Y}{N_B N_T \Delta\Omega \xi}$$

Preliminary angular distributions

- PTOLEMY used to calculate angular distributions
- Measured angular distributions compared to calculations and assignments made for states up to 2.5 MeV



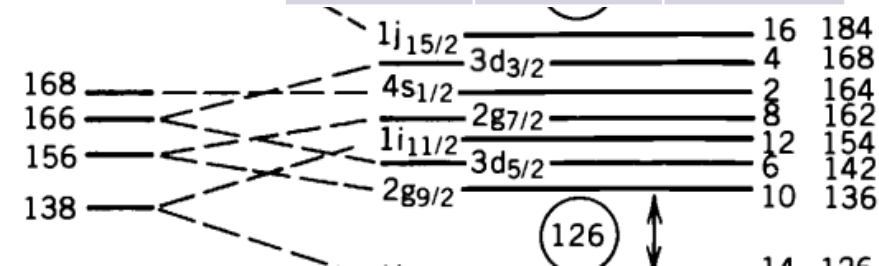
Energy / keV	L	nlj	S
0	4	2g _{9/2}	1.00(2)
681(16)	6	1i _{11/2}	2.26(23)
973(1)	2		0.31(3)
1311(5)	0	4s _{1/2}	0.27(2)
1462(10)	2		0.08(1)
1758(2)	2		0.27(1)
1937(4)	0	4s _{1/2}	0.37(1)
2132(4)	0	4s _{1/2}	0.22(1)
2380(3)	2		0.22(1)
2551(5)	2		0.17(1)

- Relative spectroscopic factors extracted by comparing with DWBA calculations
- Summed strength should equal one for a completely empty orbital as is outside a closed shell

$$\left(\frac{d\sigma}{d\Omega}\right)_{\text{exp}} = S_{ij} \left(\frac{d\sigma}{d\Omega}\right)_{\text{DWBA}}$$

- *Normalized to the 2g_{9/2} ground state

L	Orbital	Sum SF
0	4s _{1/2}	0.86(2)
2		1.05(4)
4	2g _{9/2}	1.00(2)



- New states identified in ^{213}Rn
- Preliminary spin-parity assignments have been made up to 2.5 MeV
- Extracted relative spectroscopic factors for these states
- Some work to do to extract spectroscopic information for high-lying states above 2.5 MeV
- Determine effective single-particle energy centroids and characterise how they are changing along $N=127$
- Compare to modern shell-model calculations



Kinematic Compression:

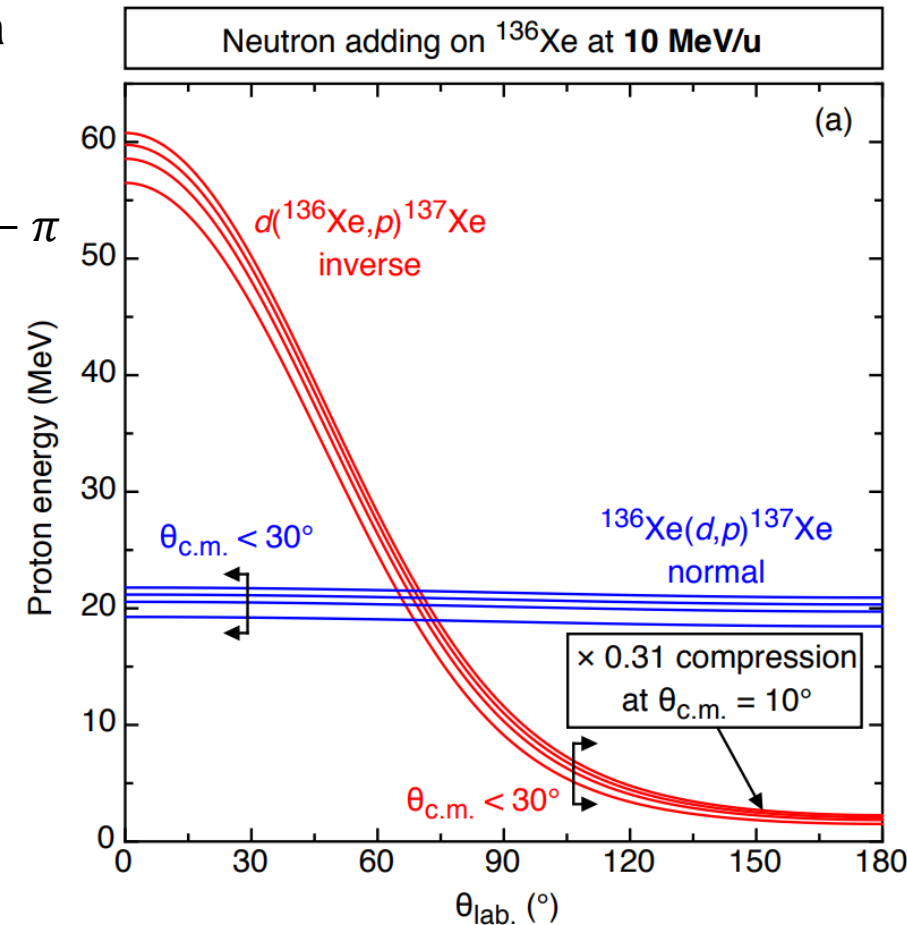
- In IK, the difference in ejectile energy for two states separated by a given excitation energy are compressed together more than in NK.

$$\Delta T_3 = A + B \sqrt{\frac{m_1}{m_2}} \cos \theta_{cm} = A - B \sqrt{\frac{m_1}{m_2}} \cos \eta_{cm} \quad \eta_{cm} = \theta_{cm} - \pi$$

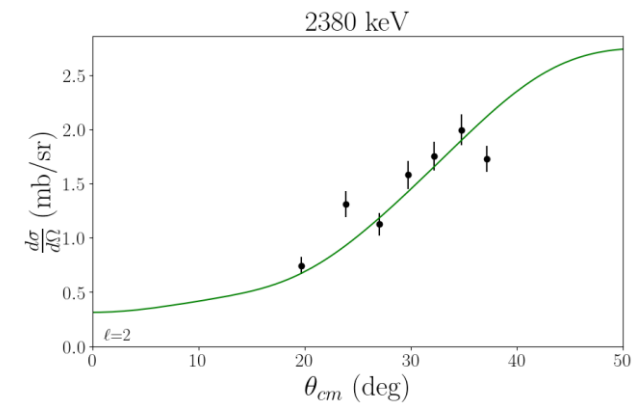
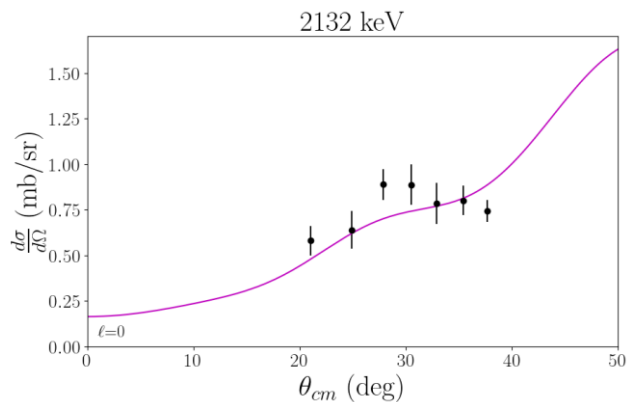
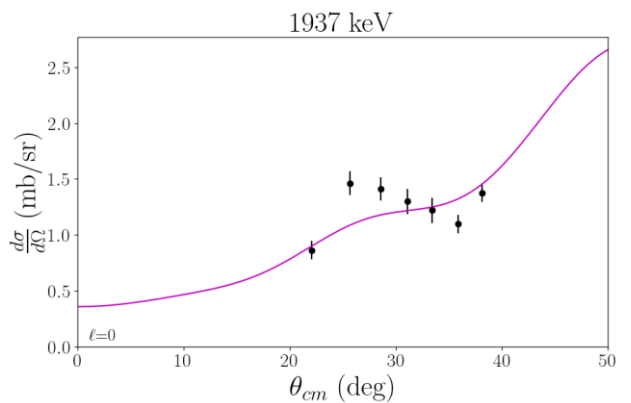
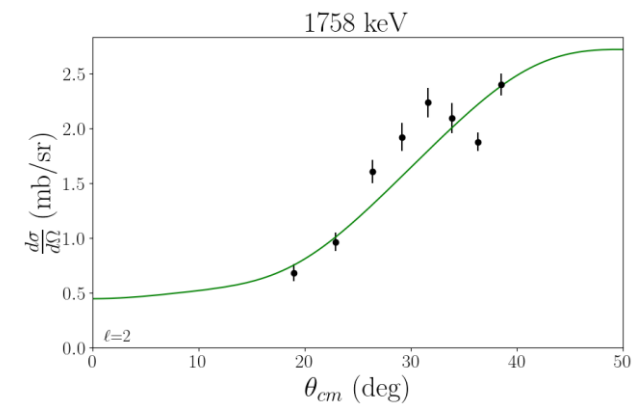
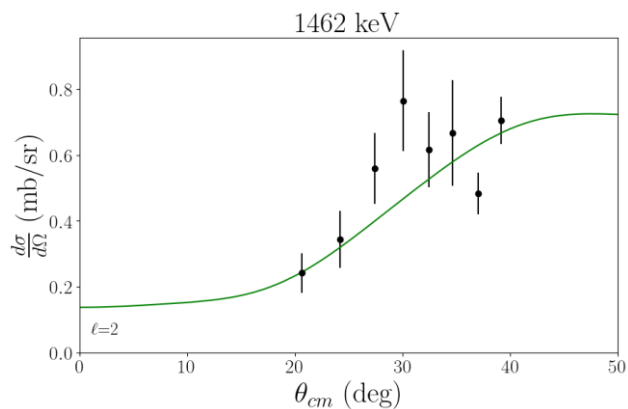
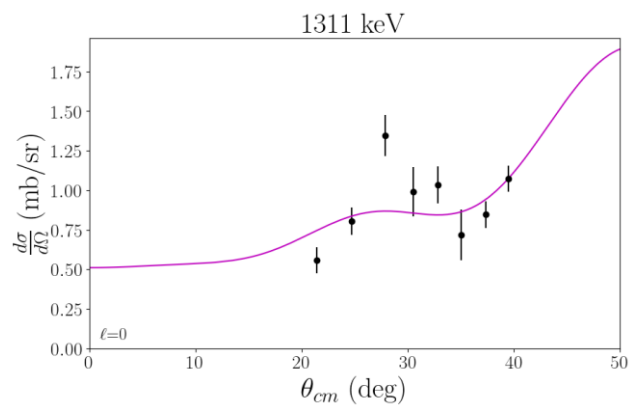
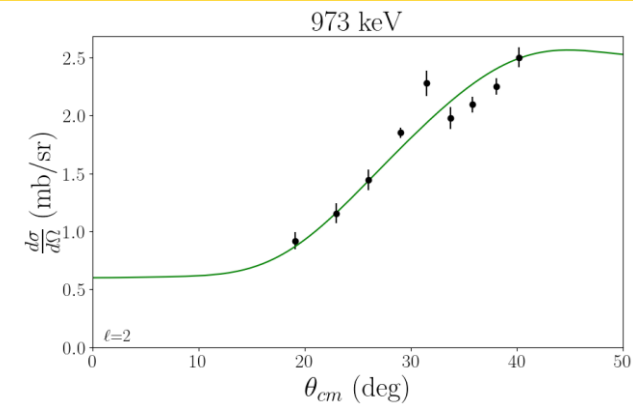
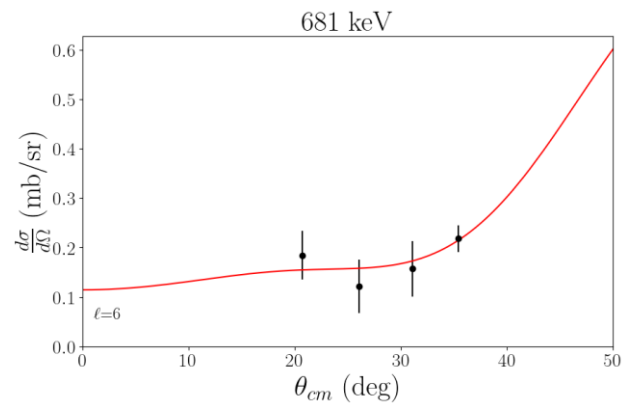
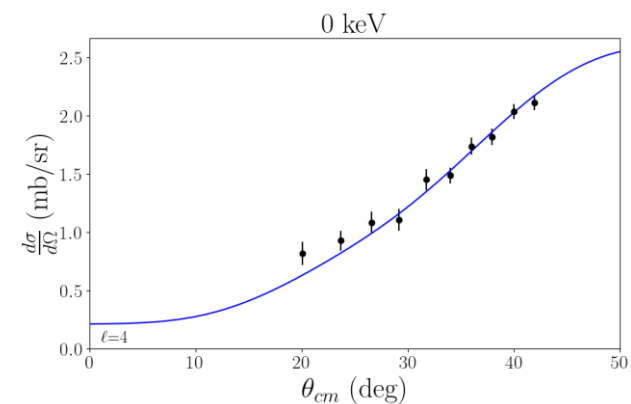
- Both NK and IK experience this with increasing CoM angle.
- Mass ratio means the affect is worse for IK and states in NK are less affected at small θ_{cm} whereas IK are affected much more at η_{cm} .

Kinematic Shift:

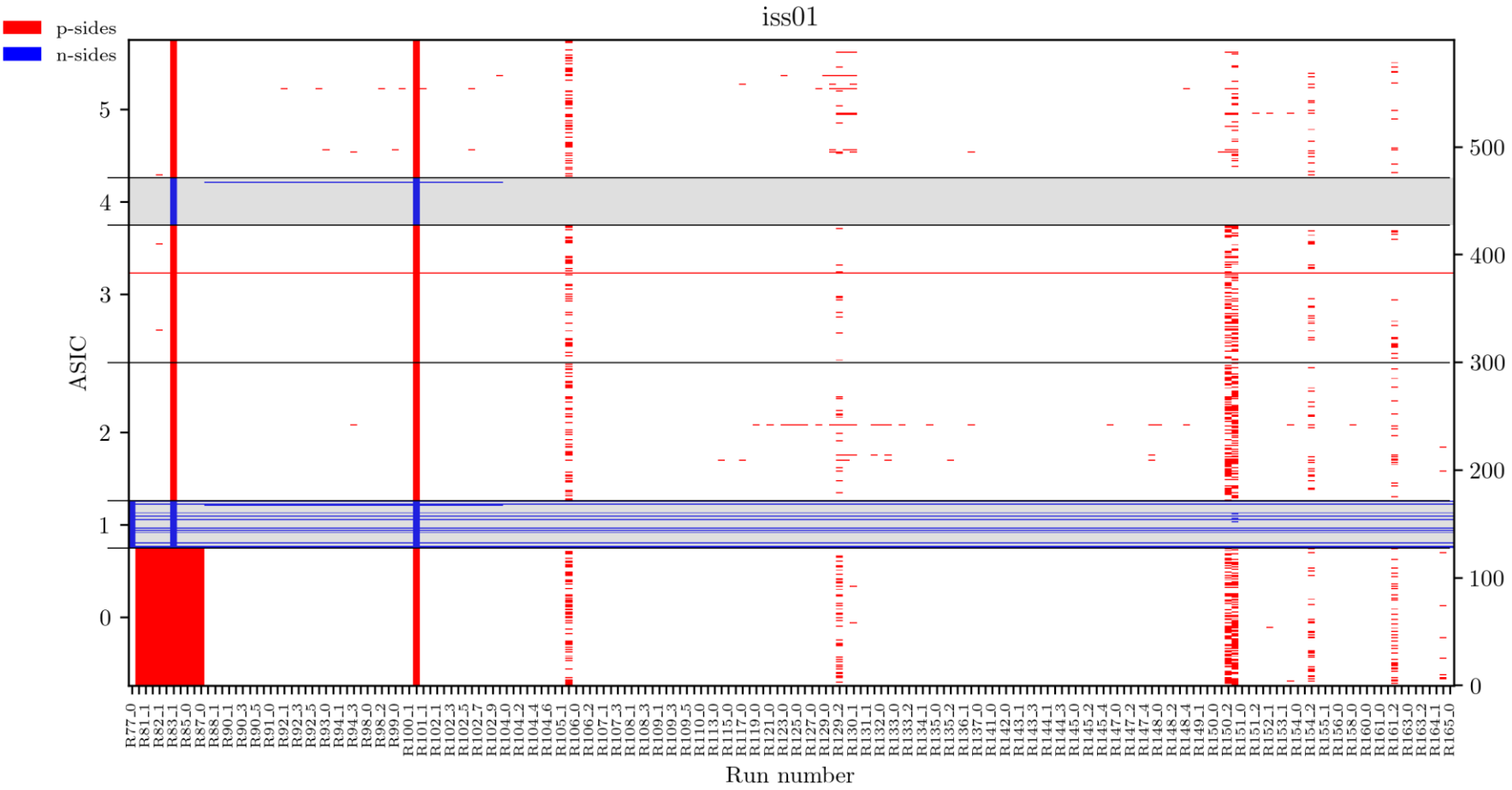
- Gradient of proton energy with angle is greater in the inverse case when compared to NK
- Finite angular acceptance allows detection of a range of energies. Peaks are broader in IK



Preliminary angular distributions

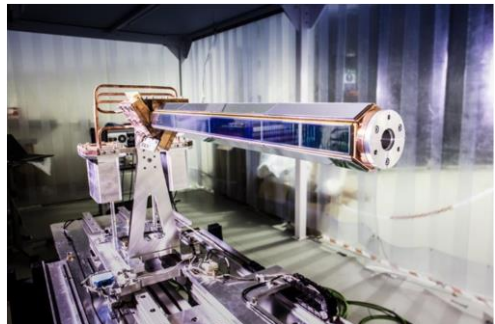
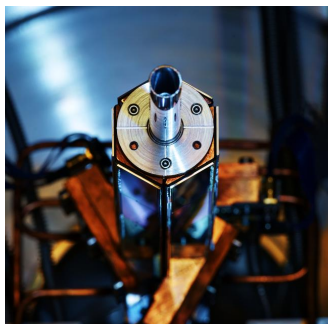


Solid angle corrections



$$\epsilon_p = \frac{\sum_i \left(\frac{\sum_j I_{ij} N_j}{\sum_j N_j} \right)}{N_p} = \frac{\sum_i \left(\frac{\sum_j I_{ij} N_j}{N_{ELUM}} \right)}{N_p}$$

$$\epsilon_n = \frac{\sum_i \left(\frac{\sum_j I_{ij} N_j}{\sum_j N_j} \right)}{N_n} = \frac{\sum_i \left(\frac{\sum_j I_{ij} N_j}{N_{ELUM}} \right)}{22}$$



- Calculations for the ground state
- Intrinsic Si energy resolution was 45-50 keV for alphas
- Target-energy loss:
 - CD2 Stopping power $\approx 160 \text{ MeV/mgcm}^2$
 - Target thickness $\approx 125 \mu\text{g/cm}^2$
 - Beam entering = 1618 keV, Beam leaving $\approx 1598 \text{ MeV}$
 - 74 keV proton energy difference in lab \Rightarrow **145 keV** excitation difference at $\theta_{\text{CM}} = 40^\circ$
- Beam spot size $\approx 3\text{mm}$:
 - Particles ejected above the beam axis due to beam spot size return to axis at a higher z than those on axis.
- Beam energy spread of $\pm 0.4 \%$ $\Rightarrow 7.63(3) \text{ MeV/u}$:
 - $E_{\text{Beam}} = 7.60 \Rightarrow 7.66 \text{ MeV/u}$
 - $\theta_{\text{CM}} = 10^\circ$; proton $\Delta E_{\text{lab}} = 12 \text{ keV}$
 - $\theta_{\text{CM}} = 40^\circ$; proton $\Delta E_{\text{lab}} = 50 \text{ keV}$

Contribution to energy resolution	At 10 degrees CM (keV)	At 40 degrees CM (keV)
Target-energy loss	50	145
Intrinsic silicon energy	50	50
Position resolution 1mm	15	15
Beam spot 3mm	88	8
Beam energy spread $\pm 0.4\%$	12	50
Total in quadrature	115	162